Pol. J. Environ. Stud. Vol. 31, No. 5 (2022), 4071-4084
DOI: *10.15244/pjoes/148190* ONLINE PUBLICATION DATE: 2022-06-20

Original Research

Hydrochemical Characteristics and Quality Assessment of Shallow Groundwater in Poultry Farming Sites in Suzhou City, China

Jiayu Chen[1,2], Herong Gui[2]*, Chen Li[1,2], Chunlei Wang[1,2], Chen Chen[1,2], Yaqi Jiang[1,2]

[1]School of Earth and Environment, Anhui University of Science and Technology, Huainan, 232001, Anhui, China
[2]National Engineering Research Center of Coal Mine Water Hazard Controlling (Suzhou University), Suzhou, 234000, Anhui, China

Received: 17 February 2022
Accepted: 9 April 2022

Abstract

In recent years, the impact of the excrement from large-scale poultry farms on the quality of shallow groundwater has attracted widespread attention. In the present study, the hydrogeochemical characteristics of shallow groundwater around poultry farming sites in the town of Zhuxianzhuang in Suzhou, Northern Anhui, China, were investigated using various statistical techniques, a Piper trilinear diagram, ion combination ratios, correlation analysis, and a fuzzy comprehensive evaluation method. The results show that the shallow groundwater in the area is dominantly of the HCO_3–Ca type. The relative abundances of the major cations and anions in the groundwater are in the order Na^+>Ca^{2+}>Mg^{2+} >K^+ and HCO_3^- >Cl^->SO_4^{2-}>NO_3^-> F^-, respectively. According to the concentrations and distribution of tri-nitrogen in the groundwater, pollution is mainly associated with domestic wastewater, followed by poultry farm waste. The most severe pollution involves NO_2–N, and this adversely impacts the potability of the shallow groundwater. The leaching of rocks and silicate weathering are the principal processes responsible for the ionic composition of the shallow groundwater in the study area. Class I, II, and III waters account for 9.52%, 28.57%, and 61.90%, respectively, of the groundwater in the area. The shallow groundwater is suitable for high salinity-tolerant plants or soils associated with good leaching conditions. Future water management in the poultry farming area should prioritize the control of shallow groundwater nitrite pollution.

Keywords: poultry farming sites, shallow groundwater, hydrochemical characteristics, water quality assessment, Zhuxianzhuang Town of Suzhou City

*e-mail: guiherong@163.com

Introduction

Owing to the development of large-scale intensive poultry farms, the surrounding environment, especially the quality of shallow groundwater, is commonly affected. In fact, approximately 3.8 billion tons of manure associated with animals are produced in China annually [1]. In addition to the high organic matter content in undigested feed, including proteins, amino acids, and other nitrogen-containing substances, manure from poultry usually contains high concentrations of trace elements and agents of infection [2-3]. In the absence of effective management, the groundwater resources surrounding the source areas of such manure are susceptible to pollution [4]. Shallow groundwater, which is closest to the surface, is easily influenced by the superficial environment; however, it is a crucial resource utilized for irrigation, aquaculture, and domestic needs. Therefore, the pollution of shallow groundwater resources through the superficial environment directly affects the health of residents in the impacted areas. Thus, knowledge of the hydrogeochemical characteristics and quality of shallow groundwater is crucial for the preservation of this resource and the rational operation of poultry farming sites.

Several studies on groundwater and the pollution associated with poultry farming sites have been conducted previously. Cruz et al. [5], for example, reported that shallow groundwater quality degradation in northern Argentina was linked to poultry farming based on the monitoring of quality parameters, including microbiological aspects. Kim et al. [6] investigated the relationship between hydrochemical processes in shallow groundwater and poultry farms in Korea based on the relationship between the Ca^{2+}+Mg^{2+} and HCO_3^- concentrations and principal component analysis (PCA), and indicated that nitrate pollution from the farms enhanced the weathering of aquifers, which increased the salinity of the groundwater. In addition, studies on the environmental impact of poultry farms on surface water in areas around poultry farms [7] and the pollution characteristics of heavy metals, nitrogen, and phosphorus in poultry manure [8-9] have also been conducted.

In the present study, poultry farming sites in the town of Zhuxianzhuang in Suzhou, Anhui Province, China, were selected and the hydrogeochemical characteristics and quality of the shallow groundwater around these sites were investigated. Suzhou, which covers an area of 9,787 km^2, is a major city in the north of Anhui Province and hosts a population of 6.58 million, with agriculture as one of the principal activities in the area. In fact, agriculture and poultry farming are the primary activities in the town of Zhuxianzhuang in Suzhou. The poultry farms involve mainly semi-industrial and industrial production systems, and degradation in septic tanks is the primary method for the treatment of poultry waste. Moreover, shallow groundwater is the main source for irrigation, poultry breeding, and domestic requirements in the area.

The major objectives of the present study were to: (1) determine the hydrochemistry of the shallow groundwater in the impact zones of poultry farming sites; (2) evaluate the water quality of the shallow groundwater at the poultry farming sites against recognized standards; and (3) investigate the tri-nitrogen characteristics of poultry farming and their relationship with groundwater quality.

Materials and Methods

Study Area

The poultry farming sites in Zhuxianzhuang are in the east of Suzhou (Fig. 1b), and these can be partitioned into two major farms (X00 and X05). The study area is between the longitudes 117°4′4” and 117°10′44” E and latitudes 33°33’16” and 33°37’46” N. The X00 poultry farm covers an area of 30000 m^2, and accounts for more than 15,000 chickens annually. The X05 poultry farm is approximately 2.4 km to the northeast of the X00 farm and covers an area of approximately 1000,000 m^2; more than 10,000 chickens are produced by the farm annually.

The study area is characterized by a typical warm temperate semi-humid monsoon climate, involving a hot and rainy summer. The average, maximum, and minimum annual temperatures in the area are 14.6, 40, and –12.5ºC, respectively, while the annual rainfall varies between 774 and 855 mm, and the annual mean evaporation is 832.4 mm [10].

Loose Quaternary sediments in the area are 200-300 m thick. These sediments host four aquifers from top to bottom. The first aquifer, which is the shallowest, exhibits a mean thickness of 30 m, and it comprises silty and fine sands as well as clay. The groundwater in this aquifer is referred to as “shallow groundwater” and occurs at depths of 3-5 m from the surface [10-11].

Sampling and Measurements

Water samples were collected from 21 household wells in the study area in August 2020. The sampling and preservation of the water samples were conducted in accordance with the procedures in the Groundwater pollution investigation and evaluation specifications (DD2008-01) and Water and wastewater detection and analysis methods (Fourth Edition). The wells were pumped for 5 min before sampling to collect fresh samples and the sampling bottles were washed thrice using the well water. After sampling, the bottles were sealed, transported to the laboratory, and stored at 4ºC for subsequent testing. The electrical conductivity (EC), pH, and total dissolved solids (TDS) were measured in situ via a portable OHAUS instrument (Shanghai,

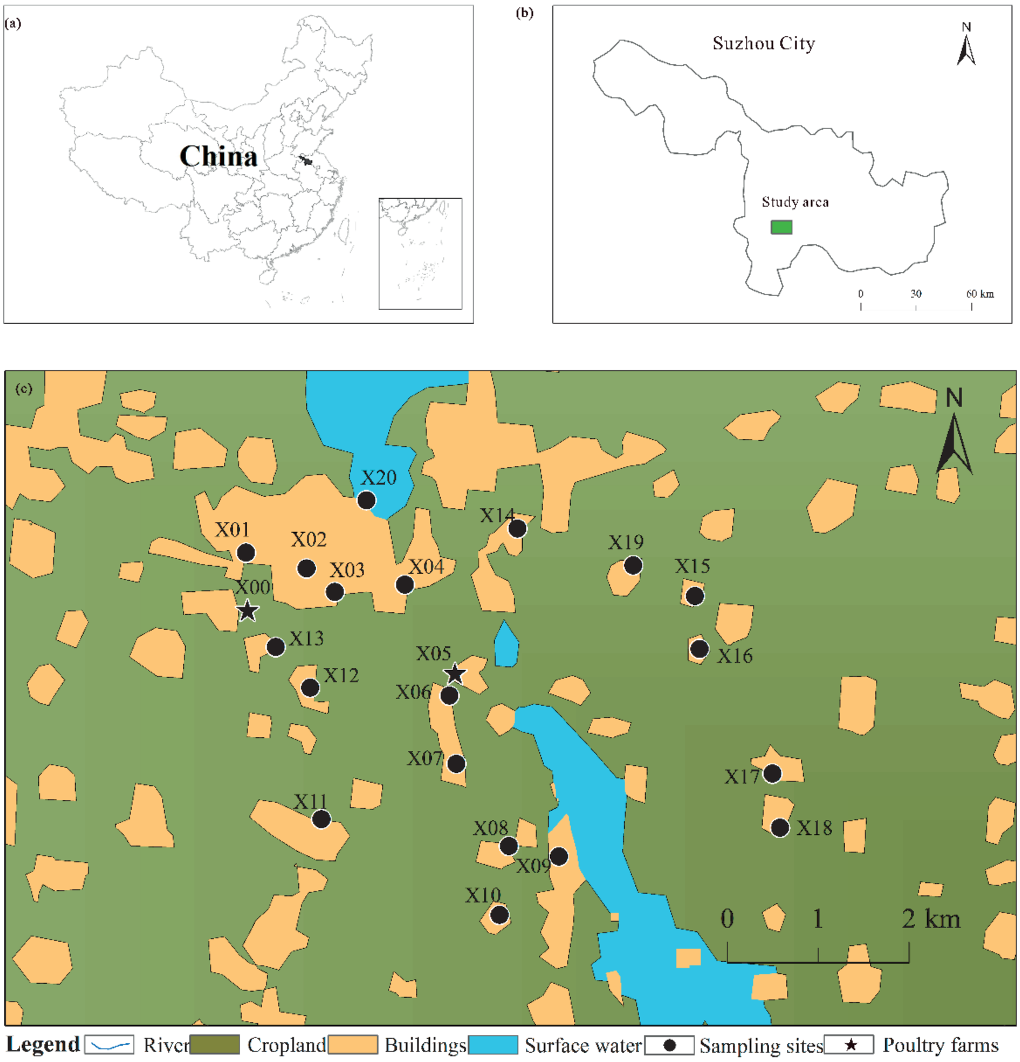

Fig. 1. Maps showing a) the location of the study area in China, b) an expanded version of the inset in a), and c) the expanded study area showing the farm and water sampling sites in Zhuxianzhuang.

China), while the locations of the sampling sites were obtained using a GPS.

Twenty-one 50-mL polyethylene bottles were used to store filtered (0.22 µm Millipore membrane filter) water samples for the measurement of dissolved ions. Analyses of Na^+, K^+, Ca^{2+}, Mg^{2+}, Cl^-, F^-, SO_4^{2-} were performed using ion chromatography (ICS-600-900), while the HCO_3^- concentration was determined using acid–base titration. The oxygen (^{18}O) and deuterium (D) isotope compositions of the groundwater samples were measured using an LGR-LWIA-45EP. The concentrations of nitrate (NO_3–N), nitrite (NO_2–N), and ammonium (NH_4–N) were analyzed using ultraviolet spectrophotometry, spectrophotometry, and Nessler's Reagent Spectrophotometry, respectively. The total nitrogen (TN), total phosphorus (TP), and chemical oxygen demand (COD) were determined using the potassium persulfate digestion ultraviolet spectrophotometry, ammonium molybdate spectrophotometry, and dichromate methods, respectively. Ten percent of the samples were analyzed in duplicate, and the associated errors were <5%.

Analytical Methods

Quality Assessment of Irrigation Water

The sodium percentage (%Na) is used to highlight the alkali hazard, because the replacement of calcium and magnesium with excess sodium in irrigation causes poor soil drainage [12]. The Na% was calculated based on the following expression:

$$Na\,\% = \frac{Na^+}{Na^+ + Ca^{2+} + Mg^{2+} + K^+} \times 100 \tag{1}$$

The sodium adsorption ratio (SAR) is employed to characterize the suitability of water for irrigation. It reflects the alkali/sodium hazard for crops [13], and is determined using the following equation:

$$SAR = \frac{Na^+}{\sqrt{(Ca^{2+}+Mg^{2+})/2}} = \frac{Na^+}{\sqrt{(Ca^{2+}+Mg^{2+})/2}} \quad (2)$$

where all concentrations are expressed in meq/L.

Fuzzy Comprehensive Evaluation

To assess the quality of the water samples for drinking, fuzzy comprehensive evaluation was employed. In general, the membership function is a useful technique for quantifying and classifying the quality of water [12, 14]. The membership functions for the water quality in different classes are expressed as follows:

Class I (j = 1):

$$r_{i1} = \begin{cases} 1 & (c_i \le s_{ij}) \\ \frac{s_{ij+1}-c_i}{s_{ij+1}-s_{ij}} & (s_{ij} < c_i < s_{ij+1}) \\ 0 & (c_i \ge s_{ij-1}) \end{cases} \quad (3)$$

Class II to Class IV (j = 2, 3, 4):

$$r_{i1} = \begin{cases} \frac{c_i-s_{ij-1}}{s_{ij}-s_{ij-1}} & (s_{ij-1} < c_i < s_{ij}) \\ 0 & (c_i \le s_{ij}, c_i \ge s_{ij+1}) \\ \frac{s_{ij+1}-c_i}{s_{ij+1}-s_{ij}} & (s_{ij} < c_i < s_{ij+1}) \end{cases} \quad (4)$$

Class V (j = 5):

$$r_{i1} = \begin{cases} 1 & (c_i \ge s_{ij-1}) \\ \frac{c_i-s_{ij-1}}{s_{ij}-s_{ij-1}} & (s_{ij-1} < c_i < s_{ij}) \\ 0 & (c_i \le s_{ij}) \end{cases} \quad (5)$$

where r_{ij} represents the fuzzy membership of indicator i to class j, c_i is the measured value of indicator i, and s_{ij} denotes the standard value of indicator i to class j.

The R matrix of n * 5 is expressed as follows:

$$R = \begin{Bmatrix} r_{11} & r_{12} & \dots & r_{1n} \\ r_{21} & r_{22} & \dots & r_{2n} \\ \dots & \dots & \dots & \dots \\ r_{m1} & r_{m2} & \dots & r_{mn} \end{Bmatrix} \quad (6)$$

while the weight expression of each indicator is obtained from the following expression:

$$W_i = \frac{c_i}{s_i} \quad (7)$$

where w_i is the weight of water quality indicator i and s_i is the average value of indicator i for Classes I to V.

The normalized weight is then expressed as follows:

$$a_i = \frac{c_i}{s_i} / \sum_{i=1}^{m} \frac{c_i}{s_i} = W_i / \sum_{i=1}^{n} W_i \quad (8)$$

where a_i is the normalized weight of indicator i and $\sum_{i=1}^{n} W_i$ represents the sum of weights for all water quality indicators. The normalized results are listed in matrix A, while the water quality evaluation was achieved through the fuzzy membership calculation of matrix B, as expressed in Eqs (9) and (10)

$$A = [\, a_1\, a_2 \cdots a_n] \quad (9)$$

$$B = A \cdot R \quad (10)$$

According to the values obtained from matrix B, the class of the water quality is determined from the order of the maximum value.

Statistical Analysis

ArcGIS 10.5 was used to produce a map of the study area indicating the locations of the water sampling sites. AqQA software (version 1.5) was utilized to construct the Piper diagrams, while the statistical analysis of the water chemistry data was performed using OriginPro 9.1 and R 4.0.3.

Results and Discussion

Hydrogeochemical Characteristics

Descriptive statistics were employed to highlight the characteristics of the water chemistry parameters. As presented in Table 1, the pH values for the water samples range from 7.39 to 9.37 (mean = 7.79), and these indicate an overall weakly alkaline character for the shallow groundwater in the region. The TDS values, which vary from 360 to 795 mg/L (mean = 558.16 mg/L), are within the limits recommended by the World Health Organization drinking water quality standard (1000 mg/L) [15] and Chinese national standard GB 5749-2006 (1500 mg/L) [16]. Therefore, the shallow groundwater in the study area is suitable for drinking. The concentrations of Ca^{2+}, Mg^{2+}, Na^+, and K^+ correspondingly range from 31.39 to 106.45 mg/L (mean = 56.63 mg/L), 20.11 to 75.14 mg/L (mean = 40.53 mg/L), 21.82 to 187.37 mg/L (mean = 86.05 mg/L), and 0 to 0.70 mg/L (mean = 0.09 mg/L). The concentrations of F^-, Cl^-, SO_4^{2-}, HCO_3^-, and NO_3^- range from 0.76 to 2.76 mg/L (mean = 1.37 mg/L), 4.88 to 181.54 mg/L (mean = 66.31 mg/L), 19.06 to 162.79 mg/L (mean = 46.30 mg/L), 382.06 to 700.44 mg/L (mean = 498.80 mg/L), and 0 to 102.63 mg/L (mean = 9.94 mg/L), respectively. In addition, the TN values range from 0 to 1801.78 mg/L (mean = 132.01 mg/L), while the COD values vary from 0 to 12.04 mg/L (mean = 4.44 mg/L).

Based on the average concentrations, the shallow groundwater in the study area is dominated by Na^+ and HCO_3^-. The measured data reveal that the major cations are in the order $Na^+ > Ca^{2+} > Mg^2 > K^+$, while the anions follow the order $HCO_3^{-}>Cl^{-}>SO_4^{2-}>NO_3^{-}>F^{-}$. In general, Na^{+} in the groundwater is attributed to the dissolution of sodium-containing minerals and/or ion exchange [17].

Similar assessments of shallow groundwater quality at poultry farms sites have been conducted in other parts of the world [6, 18-20], and the results are listed in Table 2. Except for K^{+}, the concentrations of other cations (Na^{+}, Ca^{2+}, and Mg^{2+}) in this study are higher than those in Ordos Basin, Netherlands, South Korea, and Young-am City. The concentrations of HCO_3^{-}, Cl^{-}, and F^{-} in other areas are lower than those in this study, whereas the concentration of SO_4^{2-} in the Netherlands [19] is 3.5 times higher than that in this study. The concentrations of NO_3^{-} in Young-am City, South Korea [20], and South Korea [6] are 5.3 and 3.3 times that in this study, respectively. The concentration of NO_3^{-} in this study is 2.6 times that in the Netherlands [19]. The concentration of NO_3-N in the Ordos Basin is 4.7 times higher than that in this study. The concentration of NH_4-N in this study is not different to that in the Netherlands [19], but higher than that in Young-am City [20] and the Ordos Basin [18]. This shows that the hydrochemical components of the shallow groundwater in this study are affected by human activities.

The Piper diagram created to provide a hydrochemical classification [21-23] of the samples is shown in Fig. 2. The data for cations in the shallow groundwater samples from the study area are mainly in zone B, while the data for anions are plotted principally in zone E. Based on this diagram, the groundwater samples from the study area are mainly of the HCO_3–Ca type (90.48%).

According to the coefficient of variation (CV), the water quality parameters are in the order TN>NO_3^{-}> NO_3–N>K^{+}, and their values of > 00 indicate that these parameters are susceptible to external contributions [24]. Considering the paucity of natural NO_3^{-} in rocks, an NO_3^{-} concentration of >5 mg/L usually indicates pollution from animal waste, fertilizer, or wastewater [17]. NO_3–N generally originates from the sewage of poultry farms, municipal wastewater discharge, fertilizers, and the atmosphere [25].

Correlation Analysis of Ions

Correlation analysis is valuable for highlighting elements from identical or similar sources [26]. In Fig. 3, Ca^{2+} and Mg^{2+} exhibit strong positive correlations with SO_4^{2+}, indicating that, in the groundwater in the study

Table 1. Descriptive statistics of the sample parameters.

Samples	Mean	Min	Max	S.D	CV (%)
Ca^{2+}	56.63	31.39	106.45	20.49	36.18
Mg^{2+}	40.53	20.11	75.14	14.03	34.61
Na^{+}	86.05	21.82	187.37	39.16	45.51
K^{+}	0.09	0.00	0.70	0.21	225.85
F^{-}	1.37	0.76	2.76	0.49	35.78
Cl^{-}	66.31	4.88	181.54	60.73	91.58
SO_4^{2-}	46.30	19.06	162.79	33.12	71.54
HCO_3^{-}	498.80	382.06	700.44	99.62	19.97
NO_3^{-}	9.94	0.00	102.63	25.44	255.97
NO_3-N	1.91	0.00	17.98	4.58	239.07
NO_2-N	1.33	0.45	2.73	0.67	50.76
NH_4-N	0.25	0.05	0.63	0.16	66.27
pH	7.79	7.39	9.37	0.40	5.08
TDS	558.16	360	795	136.57	24.47
EC	966.24	616	1313	241.53	25.00
TN	132.01	0.00	1801.78	427.24	323.63
COD	4.44	0.00	12.04	3.94	88.63
$\delta^{18}O$	−7.50	−8.41	−6.49	0.57	−7.60
$\delta^{2}H$	−51.63	−56.27	−46.29	3.13	−6.07

Units: Ion concentration (mg/L), TDS (mg/L), EC (μS/cm), S.D indicates the standard deviation, CV indicates the coefficient of variation.

Table 2. Comparison of parameters contents in shallow groundwater in different poultry farming areas (Unit: mg/L, expect for pH and EC).

Site	K^+	Na^+	Ca^{2+}	Mg^{2+}	HCO_3^-	SO_4^{2-}	Cl^-	F^-	NO_3^-	NO_3-N	NH_4-N	pH	TDS	EC	Reference
Suzhou City	0.09	86.05	56.63	40.53	498.80	46.30	66.31	1.37	9.94	1.91	0.22	7.79	558.16	966.24	This study
Ordos Basin	2.08	44.51	47.99	14.93	234.8	32.45	24.91	0.31	-	8.99	0.05	8.05	328	494.0	[18]
Netherlands	-	18.35	32.79	10.17	5.03	161.75	30.34	-	3.80	-	0.27	5.10	-	-	[19]
South Korea	2.4	16.2	25.6	6.2	72.3	13.3	20.9	-	32.9	-	-	5.7	189.7	138.8	[6]
Young-am City	2.05	25.50	18.48	5.38	34.22	2.29	33.79	-	52.64	-	0.02	6.20	-	254.27	[20]

EC unit, μs/cm

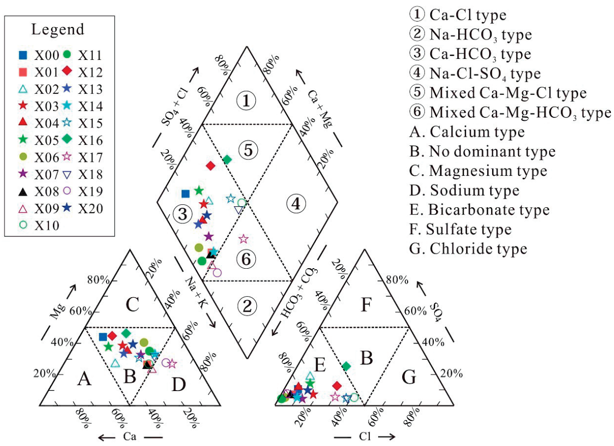

Fig. 2. Piper diagram showing the composition of shallow groundwater samples collected from the poultry farming sites.

area, these cations were probably derived from the same source. Moreover, the moderate correlation between SO_4^{2-} and NO_3–N suggests that the former originates from chemical fertilizers or pesticides. Conversely, the positive correlation between TP and K^+ indicates that, in the shallow groundwater in the study area, the former is probably derived from agricultural non-point source pollution.

Mechanisms Associated with Groundwater Composition

The principal mechanisms that control the composition of groundwater are weathering, atmospheric precipitation, and evaporation-crystallization [27]. According to the Gibbs diagram (Fig. 4), the primary mechanism responsible for the chemistry of the shallow groundwater in the study region is weathering, while dissolution enhances the concentrations of some ions. In addition, in Fig. 4a), the sample data are clustered where the $Na^+/(Na^+ + Ca^{2+})$ values generally exceed 0.5. These results suggest that the shallow groundwater in the study area is significantly impacted by the cation exchange process [28].

The relationships between the Mg^{2+}/Na^+ and Ca^{2+}/Na^+ (Fig. 5a) and HCO_3^-/Na^+ and Ca^{2+}/Na^+ (Fig. 5b) ratios for samples from the study area were examined to evaluate the impacts of silicates, carbonates, and evaporites on the composition of the groundwater [29]. Evidently, the data for most samples fall in the area associated with the weathering of silicates, and the hydrochemical characteristics of the shallow groundwater in the study area are dominantly imparted through the weathering of silicates, with a subordinate contribution from the weathering of carbonate rocks.

The molar ratios of major ions are commonly utilized to identify chemical processes associated with groundwater and evaluate the sources of dissolved ions [30-32]. For example, Na^+/Cl^- close to unity indicates that the dissolution of rock salt is the main source of Na^+

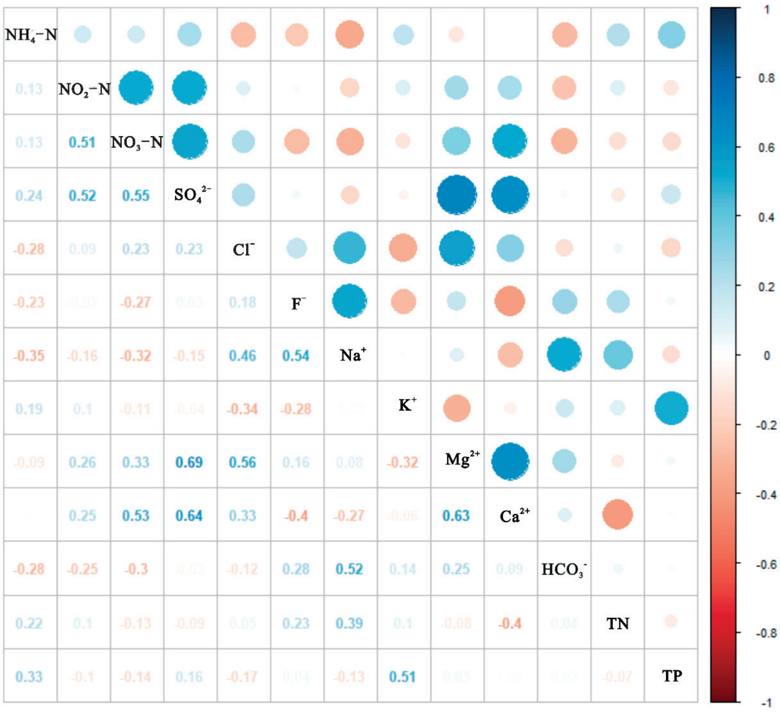

Fig. 3. Correlation chart involving 13 variables for shallow groundwater samples from the poultry farming sites.

in groundwater [30]. Conversely, a ratio of 1 implies that Na^+ is principally introduced to groundwater through the weathering of silicates [30, 33]. In the present study, the $Na^+ + K^+/Cl^-$ ratios are mostly >1 (Fig. 6a), indicating that, in addition to the dissolution of rock salt, the weathering of silicates (e.g., albite and K-feldspar) is another important source of $Na^+ + K^+$ in the shallow groundwater. Ca^{2+}/HCO_3^- ratios close to or less than 1 suggest that the weathering of calcite is the main source of these ions in groundwater [21, 33]. As shown in Fig. 6b), the data for most of the samples studied are near the 1:2 line, which indicates that the weathering of dolomite is the main contributor of Ca^{2+} and HCO_3^- in the shallow groundwater. Similarly, the dissolution of gypsum produces a Ca^{2+}/SO_4^{2-} ratio close to 1 for groundwater [31]. In the present study, the correlation

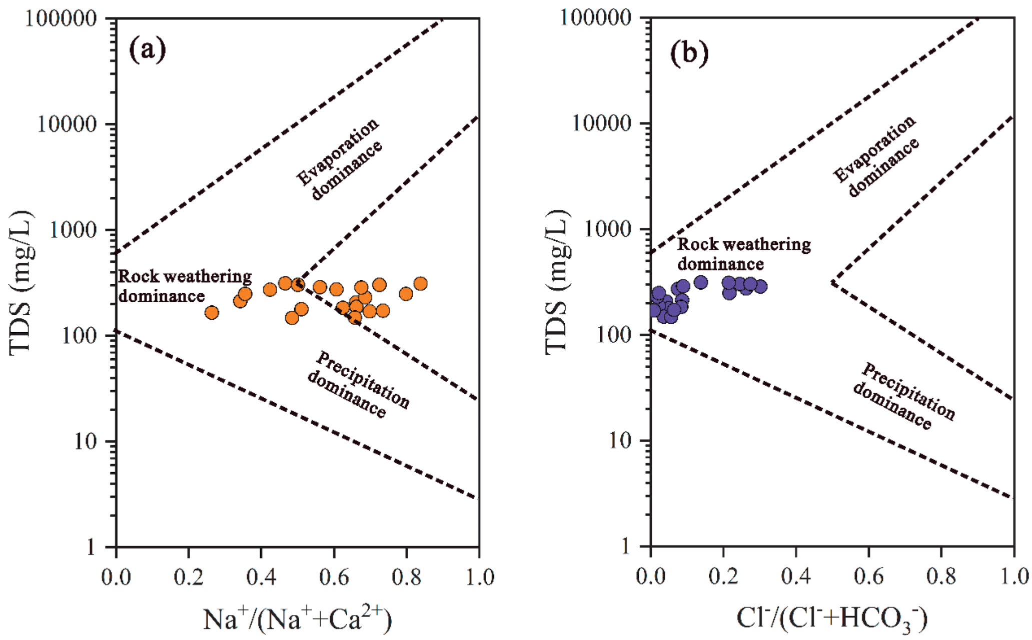

Fig. 4. Gibbs diagrams highlighting the hydrochemical processes responsible for the compositions of shallow groundwater from the poultry farming sites based on a) cations and b) anions.

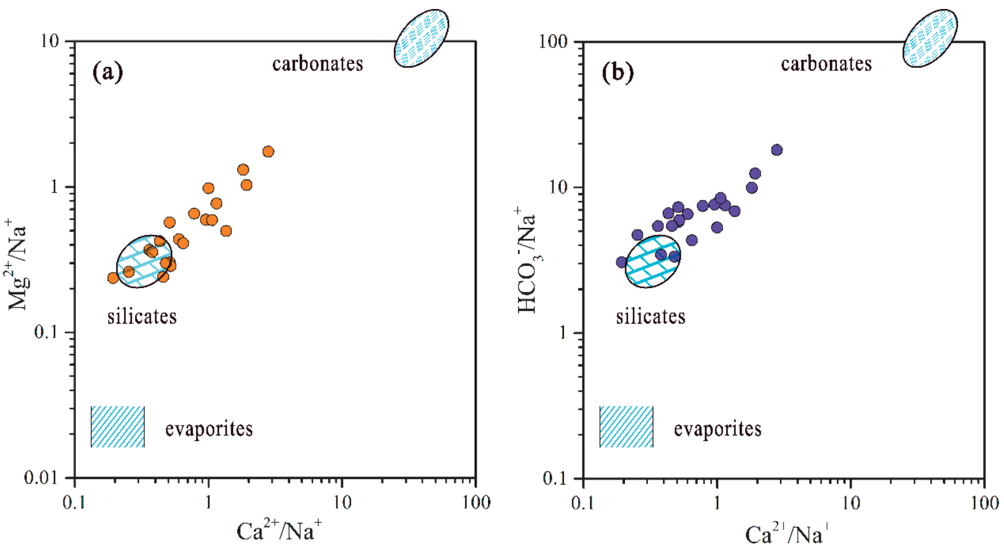

Fig. 5. Ionic ratio plots reflecting the origin of ions in shallow groundwater from poultry farming sites based on a) cations-cations and b) cations-anions.

between Ca^{2+} and SO_4^{2-} is weak (R^2 = 0.40), and the data for all samples are plotted above the 1:1 line (Fig. 6c). These results demonstrate that the dissolution of gypsum and anhydrite is not the principal mechanism responsible for the presence of these ions in the studied shallow groundwater. In addition, the dissolution of dolomite causes the Ca^{2+}/Mg^{2+} ratio to fall near the 1:1 line, while ratios close to 2 indicate higher contributions from calcite [34]. In the present study, data for only a few samples are plotted between the 1:1 and 1:2 lines (Fig. 6d). The excessive Mg^{2+} in the samples shows that, although the dissolution of dolomite contributes, it is not the main process responsible for the concentrations of Mg^{2+} in the shallow groundwater. According to Lin et al. [33], the dissolution of carbonates and sulfates produces a Ca^{2+} + Mg^{2+}/HCO_3^- + SO_4^{2-} ratio close to 1. Data for few samples in the present study are plotted near the 1:1 line, while most fall under the 1:1 line (Fig. 6e). These results rule out the dissolution of sulfate as the main process responsible for these ions in the groundwater, although the dissolution of carbonate certainly contributed [35]. The data for most samples are plotted between the 1:1 and 1:2 lines (Fig. 6f), confirming that the dissolution of carbonate is not the primary source of the Ca^{2+} and Mg^{2+} in the studied groundwater.

The ion exchange reaction can be inferred from the relationships between the Ca^{2+}+Mg^{2+}–SO_4^{2-} + HCO_3^- and Na^+ + K^+–Cl^- ions. If cation exchange reactions are involved, these ions are expected to exhibit ratios close to –1 [37]. In the present study, the strong positive correlations (R^2 = 0.95) between these ions (shown in Fig. 6g) indicate that cation exchange reactions are involved. The chlor-alkali index (CAI) reflects direct or reverse cation exchange reactions. In Fig. 6h, the data for most water samples are in the area are characterized by CAI values of <0, which indicates that the Mg^{2+} and Ca^{2+} in the shallow groundwater are associated through ion exchange reactions with the Na^+ and K^+ in rocks [35], with minimal occurrence of the opposite process. Consequently, the concentrations of Na^+ and K^+ in the groundwater are increasing, while those of Mg^{2+} and Ca^{2+} are decreasing.

Analysis of the Composition of Stable Isotopes

The δD values for the samples presented in Table 1 vary from –56.27 to 46.29‰ (–51.63‰), while those for $\delta^{18}O$ range from –8.41 to 6.49‰ (–7.50‰).

The relationship between the $\delta^{18}O$ and δ^2H for water in the atmosphere varies within a range near the global meteoric water line (GMWL), which is expressed as $\delta^2H = 8\delta^{18}O + 10$ (Craig 1961). Conversely, the local meteoric water line (LMWL) is expressed as $\delta^2H = 7.8\delta^{18}O + 8.2$ [36]. According to the relationship between $\delta^{18}O$ and δ^2H shown in Fig. 7, the water sample data are mostly under the GMWL and LMWL, which illustrates that precipitation is the main large-scale recharge source for the shallow groundwater in the study area [37-39]. In addition, the fitting of data for the water samples produced good results (R^2 = 0.64), and this further indicates that other sources contributed to the groundwater in the study area [40]. In fact, the data for samples X02, X12, and X16, which are plotted far from the GMWL and LMWL, suggest that the groundwater in these sites involves significant contributions from another source.

Overall, the relationship between the $\delta^{18}O$ and δ^2H for the shallow groundwater in the poultry farming sites in Zhuxianzhuang can be expressed as follows:

$$\delta^2H = 4.46\ (\pm\ 0.74)\ \delta^{18}O - 18.19\ (\pm\ 5.55);\ R^2 = 0.64 \quad (11)$$

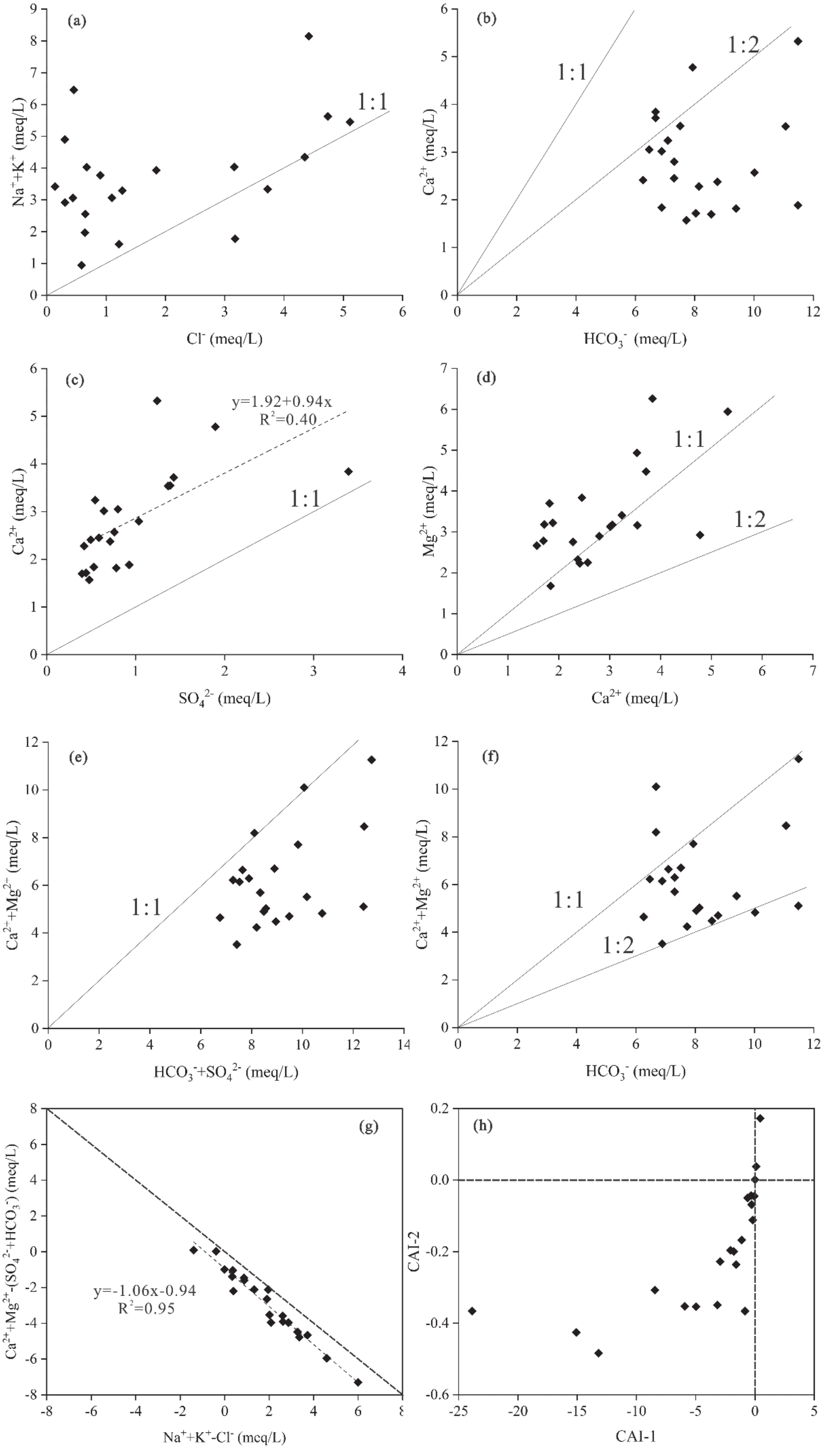

Fig. 6. Relationships between the major ions in shallow groundwater samples from poultry farming sites.

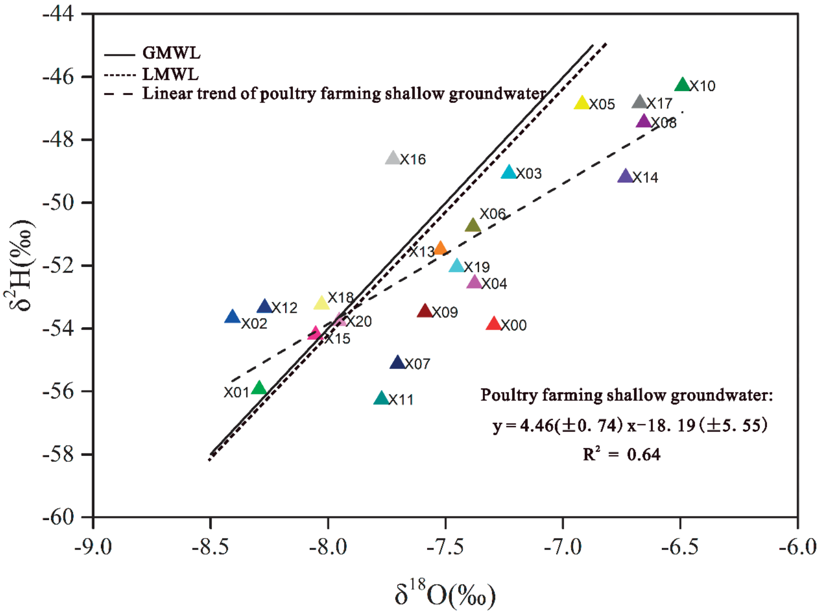

Fig. 7. Plot of δ^{18}O versus δ^2H data for shallow groundwater samples from the study area.

Water Quality Assessment

Assessment of the Water Quality for Drinking

The shallow groundwater in the study area is mainly exploited as a drinking water resource by the local residents. According to the groundwater quality standard (GB/T 14848-2017) [41] and drinking water quality standard (GB/T 5749-2006) [16], the data for the groundwater samples produce five classes (Table 3). The fuzzy comprehensive assessment (Eqs (3)–(10)) shows that the samples are categorized into Classes I, II, and III, which account for 9.52%, 28.57%, and 61.90%, respectively, of the total shallow groundwater samples (Fig. 8). This indicates that the shallow groundwater in the study area is suitable for landscape entertainment, and industrial and agricultural water use. Overall, the shallow groundwater in the study area is suitable for drinking.

Assessment of the Water Quality for Irrigation

In the study area, the shallow groundwater is also the main source of water for the irrigation of farms. Therefore, the electrical conductivity, SAR, and Na% data for the samples were plotted in USSL (Fig. 9a) [41] and Wilcox (Fig. 9b) [43] diagrams to assess the suitability of the groundwater for irrigation. According to the data in these diagrams, 21.9% (X08, X13, and X00) of the water samples are rated excellent to good for irrigation. These water samples, which fall in the C2–S1 (medium salinity and low sodium content) category, indicate that the quality of the shallow groundwater studied is suitable for plants that grow under moderate leaching conditions or possess moderate salinity tolerance [13]. The percentage representing good to permissible is 65.85%, and these samples are in the C3-S1 (high salinity and low sodium content) category. This suggests that the groundwater could be used to irrigate soils with leaching and good drainage

Table 3. Groundwater quality classification for drinking and irrigation.

Class	Cl^-	SO_4^{2-}	NH_4-N	NO_2-N	NO_3-N	Suitability
I	50	50	0.02	0.01	2	Drinking, Irrigation
II	150	150	0.10	0.10	5	Drinking, Irrigation
III	250	250	0.50	1.00	20	Drinking, Irrigation
IV	350	350	1.50	4.80	30	Irrigation
V	> 350	> 350	> 1.50	> 4.80	> 30	Not suitable

Units: Ion concentration (mg/L), TDS (mg/L).

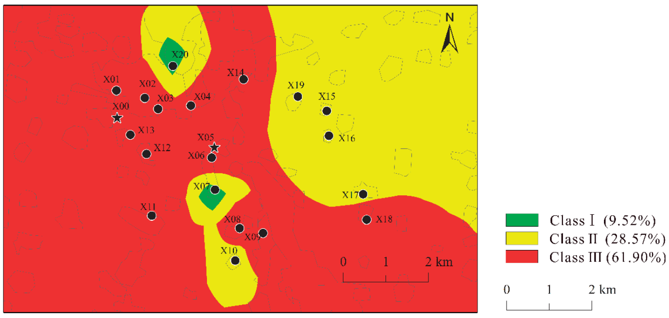

Fig. 8. Fuzzy comprehensive evaluation of shallow groundwater in poultry farming sites.

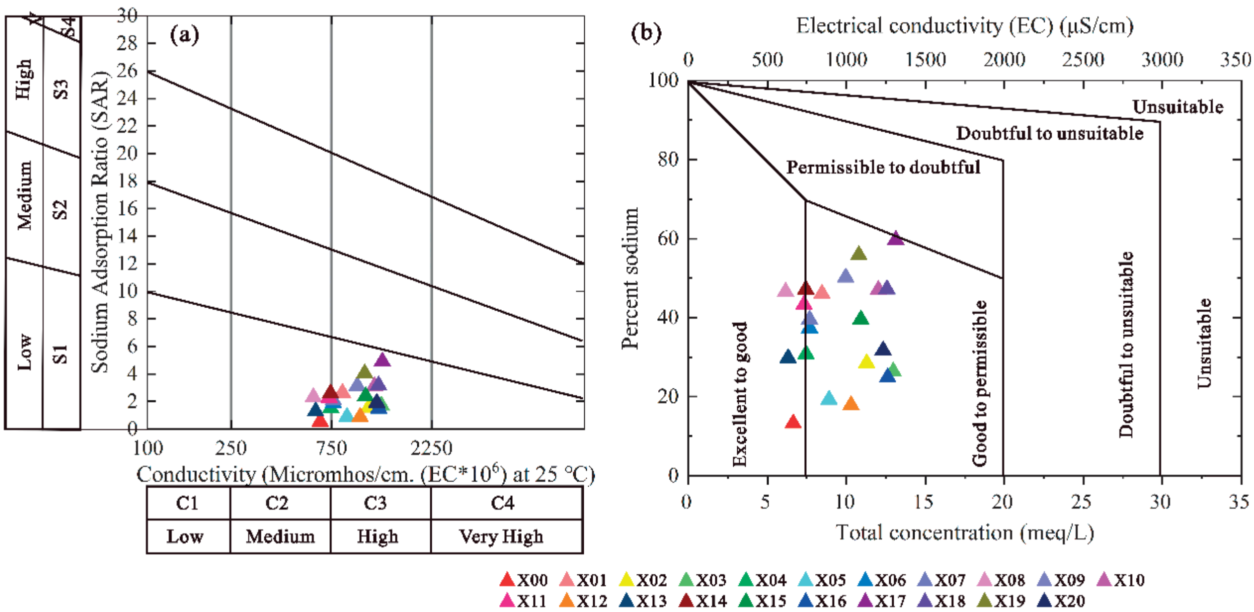

Fig. 9. a) USSL and b) Wilcox diagrams highlighting the characteristics of the groundwater samples studied.

[12]. Plants that can tolerate high salinity are required in this soil to minimize the occurrence of a salinity hazard. In general, the salinity of the groundwater in the study area requires reduction before its utilization for irrigation.

Evaluation of the Tri-nitrogen Data

Characteristics of the Tri-nitrogen Data

The concentrations of tri-nitrogen in groundwater are useful for highlighting the contribution of anthropogenic activities to the pollution of shallow groundwater in poultry farming areas. Nitrate, ammonia, and nitrite formation are associated with the decomposition of protein-containing organic matter in groundwater. Therefore, the presence of protein in groundwater indicates contamination from anthropogenic activities [31]. According to the data in Fig. 10, the NO_3–N concentrations for the samples are ≤17.98 mg/L (mean = 1.91 mg/L), while

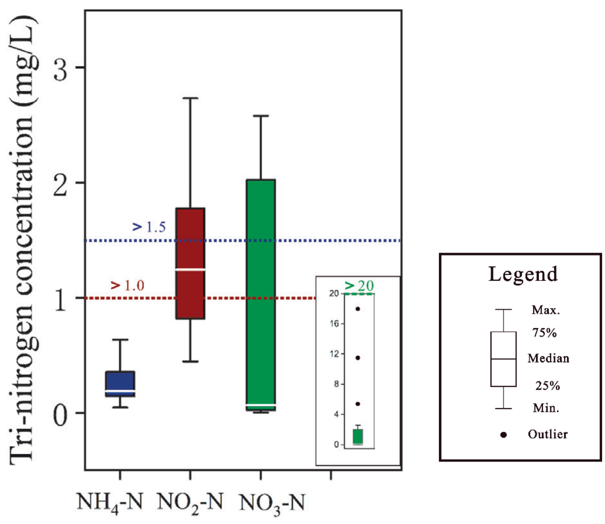

Fig. 10. Box charts of tri-nitrogen in water samples from the study area. The dotted lines in blue, red, and green represent the limits of the NH_4-N, NO_2-N, and NO_3-N concentrations, respectively, for the national standard (GB/T 14848-2017).

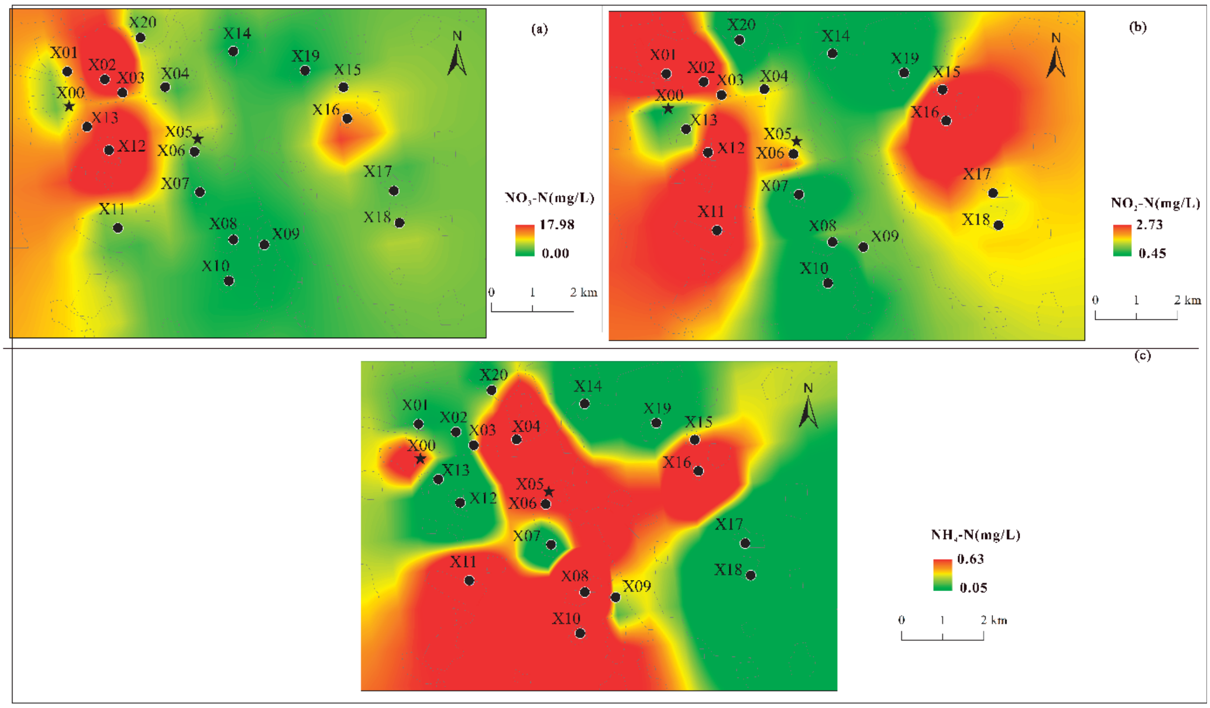

Fig. 11. Maps exhibiting the concentrations and distribution of tri-nitrogen in groundwater in the study area.

the concentrations of NO_2–N and NH_4–N range from 0.45 to 2.73 mg/L (mean = 1.33 mg/L) and 0.05 to 0.63 mg/L (mean = 0.25 mg/L), respectively. The concentrations of NO_3–N in the water samples are within the acceptable limits stated in the Chinese national standard (20 mg/L; GB/T 14848-2017), while the NO_2–N concentrations of 14 samples (>66.7%) exceed the acceptable limit of the standard (1.00 mg/L). Additionally, 9.52% of the samples show NH_4–N concentrations higher than the acceptable limit defined in the national standard (0.50 mg/L). Therefore, the most serious tri-nitrogen pollutant in the shallow groundwater of the poultry farming sites in Zhuxianzhuang is NO_2–N, followed by NH_4–N, and NO_3–N.

Distribution Characteristics of Tri-nitrogen

To further assess the contamination of shallow groundwater caused by the poultry farms, maps showing the distributions of the concentrations of NO_3–N, NO_2–N, and NH_4–N in the study area were created (Fig. 11). The concentrations of NO_3–N for most sampling sites were low (<20 mg/L), while those for NO_2–N were generally >1 mg/L. The irregular variation in the pollution involving NO_2–N originates mainly from the indiscriminate treatment and disposal of domestic wastewater, followed by the waste from the poultry farms. The concentrations of NH_4–N in groundwater in the farm sites are relatively high, and these suggest significant contamination of groundwater from the poultry farms.

The results of the drinking water quality assessment were compared with those for the spatial distribution of the tri-nitrogen concentrations. This revealed that samples X07 and X20 belong to Class I, while samples X10, X13, X15, X16, X17, and X19 are in Class II. The concentrations of NO_2–N in samples X15, X16, and X17 exceed that of the standard. All other samples fall into Class III, mainly because the concentrations of NO_2–N in samples X01, X02, X03, X04, X06, X08, X09, X11, X12, X14, and X18 exceed that of the standard. Sample X08 in Class III also exhibits an NH_4–N concentration that is higher than that of the standard. Therefore, the water quality indicators that commonly showed values higher than the limits in the standard are NO_2–N and NH_4–N. Similarly, at the site of sample X08, the reaction of carbonate and silicate rocks with NH_4^+ to produce Ca^{2+} and Mg^{2+} reduces the SAR value (see Eqs (14)), improving the quality of the shallow groundwater for irrigation.

$$Ca_{(1-x)}Mg_xAl_2Si_2O_8 + NH_4^+ + 2O_2 = (1-x)Ca^{2+} + xMg^{2+} + Al_2Si_2O_5(OH)_4 + NO_3^- \quad (14)$$

Conclusions

In the present study, shallow groundwater in Suzhou, China, was investigated, and the main findings are summarized as follows:

(1) The shallow groundwater in the study area was dominantly of the HCO_3–Ca type. Data for the concentrations of the major cations produced the order $Na^+ > Ca^{2+} > Mg^{2+} > K^+$, while the those of the anions yielded the order $HCO_3^- > Cl^- > SO_4^{2-} > NO_3^- > F^-$. The assessment of tri-nitrogen data revealed that the

most severe pollution was associated with NO_2–N, and this was attributed to the indiscriminate disposal of domestic wastewater. The NH_4–N pollution was closely linked to the discharge of waste from the poultry farms.

(2) The composition of the shallow groundwater in the study area was mainly affected by the leaching of rocks and weathering of silicates. Na^+ and K^+ were attributed mainly to the weathering of silicates, while Ca^{2+} was attributed to the dissolution of dolomite, and Mg^{2+}, SO_4^{2-}, and HCO_3^- originated mainly from the dissolution of sulfate. The ion exchange reactions between the Ca^{2+} and Mg^{2+} in the shallow groundwater and Na^+ and K^+ in rocks in the area also impacted the composition.

(3) The fuzzy comprehensive assessment showed that the quality of the shallow groundwater from the study area was good, and the water was suitable for landscape entertainment, and industrial and agricultural water use. Based on the quality for irrigation, the groundwater samples were in the C2–S1 (medium salinity, low Na^+ content) and C3–S1 (high salinity, low Na^+ content) categories. To prevent eventual hazards, measures to control the salinity of the groundwater are needed. The groundwater is suitable for plants with high salinity tolerance or soils with good drainage.

Acknowledgments

This work was funded by the National Natural Science Foundation of China (41773100), the Projects for Research Activities of Academic and Technological Leaders of Anhui Province (2020D239), the Research Project of the Wanbei Coal-Electri City Group Co. Ltd (2020), and the Research Project of the Huaibei Mining Group Co. (2021).

Conflict of Interest

The authors declare no conflict of interest.

References

1. XU H.J., HONG C.L., YAO Y.L., LIU L.J., WANG W.P., ZHU W.J., HONG L.D., WENG J.Q., ZHOU Y., ZHU F.X. The process of biotransformation can produce insect protein and promote the effective inactivation of heavy metals. Science of the Total Environment **776**, 145864, **2021**.
2. ZHU F.X., HONG C.L., WANG W.P., LYU H.H., ZHU W.J., XV H.J., YAO Y.L. A microbial agent effectively reduces ammonia volatilization and ensures good maggot yield from pig manure composted via housefly larvae cultivation. Journal of Cleaner Production **270**, 12237, **2020**.
3. KIM S.H., KIM H.R., YU S., KANG H.J., HYUN I.H., SONG Y.C., KIM H., YUN S.T. Shift of nitrate sources in groundwater due to intensive poultry farming on Jeju Island, South Korea: With emphasis on legacy effects on water management☆. Water Research **191**, 116814, **2021**.
4. YANG X.P., LI Q., TANG Z., ZHANG W.W., YU G.H., SHEN Q.R., ZHAO F.J. Heavy metal concentrations and arsenic speciation in animal manure composts in China. Waste Management **2017**.
5. CRUZ M.C., CACCIABUE D.G., GIL J.F., GAMBONI O., VICENTE M.S., WUERTZ S., GONZO E., RAJAL V.B. The impact of point source pollution on shallow groundwater used for human consumption in a threshold country†. Journal of Environmental Monitoring **14**, 2338, **2012**.
6. KIM H.R., YU S., OH J., KIM K.H., LEE J. H., MONIRUZZAMAN M., KIM H.K., YUN S.T. Nitrate contamination and subsequent hydrogeochemical processes of shallow groundwater in agro-livestock farming districts in South Korea. Agriculture, Ecosystems & Environment **273**, 50, **2019**.
7. SONG L., MAO H.Q., LI W.Y., GAO X.F., OU J., LI Q. Pollution characteristics and environmental quality analysis of surface water around livestock and poultry farms in the Pearl River Delta. Ecology and Environmental Sciences **29** (7), 1427, **2020**.
8. LIU W.R., ZENG D., SHE L., SU W.X., HE D.C., WU G.Y., MA X.R., JIANG S., JIANG C.H., YING G.G. Comparisons of pollution characteristics, emission situations, and mass loads for heavy metals in the manures of different livestock and poultry in China. Science of the Total Environment **734**, 139023, **2020**.
9. KEKRE K.M., ANVARI A., KAHN K., YAO Y., RONEN A. Reactive electrically conducting membranes for phosphorus recovery from livestock wastewater effluents. Journal of Environmental Management **282**, 111432, **2021**.
10. QIU H.L., GUI H.R. Heavy metals contamination in shallow groundwater of a coal-mining district and a probabilistic assessment of its human health risk. Human and Ecological Risk Assessment: An International Journal **2019**.
11. XIA Y.T., GUI H.R., ZHAO H.H., LI J., GUAN L.S. Temporal variability of hydrochemical characteristics and water quality assessment of collapse pond in Zhuxianzhuang coal mining area, China. Fresenius Environmental Bulleti **28** (1), 402, **2019**.
12. ZHANG B., SONG X.F., ZHANG Y.H., HAN D.M., TANG C.Y., YU Y.L., MA Y. Hydrochemical characteristics and water quality assessment of surface water and groundwater in Songnen plain, Northeast China. Water Research **46**, 2737, **2012**.
13. SUBRAMANI T., ELANGO L., DAMODARASAMY S.R. Groundwater quality and its suitability for drinking and agricultural use in Chithar River Basin, Tamil Nadu, India. Environmental Geology **47**, 1099, **2005**.
14. JI X.L., DAHLGREN R.A., ZHANG M.H. Comparison of seven water quality assessment methods for the characterization and management of highly impaired river systems. Environmental Monitoring and Assessment **188**, 15, **2016**.
15. Word Health Organization (WHO). Guidelines for drinking water quality, 4nd edition, Geneva, **2008**.
16. MH (Ministry of Health of the People's Republic of China). and SAC (Standardization Administration of the People's Republic of China). Standards for drinking water quality (GB 5749-2006). Beijing: Standards Press of China, **2006**.
17. LI C., GAO X.B., WANG Y.X. Hydrogeochemistry of high-fluoride groundwater at Yuncheng Basin, northern China. Science of the Total Environment **508**, 155, **2015**.
18. QIAN C., WU X., MU W.P., FU R.Z., ZHU G., WANG Z.R., WANG D.D. Hydrogeochemical characterization

and suitability assessment of groundwater in an agro-pastoral area, Ordos Basin, NW China. Environmental Earth Sciences **75** (20), 1356, **2016**.
19. KIVITS T., BROERS H.P., BEELTJE H., VLIET M.V., GRIFFIOEN J. Presence and fate of veterinary antibiotics in age-dated groundwater in areas with intensive livestock farming. Environmental Pollution **241**, 988, **2018**.
20. OH J., KIM H.R., YU S., KIM K.H., YUN S.T. Delineating the impacts of poultry burial leachate on shallow groundwater in a reclaimed agro-livestock farming area, using multivariate statistical analysis of hydrochemical data. Environmental Science and Pollution Research International **28** (7), 7742, **2021**.
21. LIU J.T., PENG Y.M., LI C.S., GAO Z.J., CHEN S.J. Characterization of the hydrochemistry of water resources of the Weibei Plain, Northern China, as well as an assessment of the risk of high groundwater nitrate levels to human health☆. Environmental Pollution **268**, 115947, **2021**.
22. WANG Z., GUO H.M., XIU W., WANG J., SHEN M.M. High arsenic groundwater in the Guide basin, northwestern China: Distribution and genesis mechanisms. Science of the Total Environment **640-641**, 194, **2018**.
23. ARMENGOL S., MANZANO M., BEA S A., MARTÍNEZ S. Identifying and quantifying geochemical and mixing processes in the Matanza-Riachuelo Aquifer System, Argentina. Science of the Total Environment **599-600**, 1417, **2017**.
24. YANG Q.C., LI Z.J., MA H.Y., WANG L.C., MARTÍN J.D. Identification of the hydrogeochemical processes and assessment of groundwater quality using classic integrated geochemical methods in the Southeastern part of Ordos basin, China. Environmental Pollution **218**, 879, **2016**.
25. JI X.L., XIE R.T., HAO Y., LU J. Quantitative identification of nitrate pollution sources and uncertainty analysis based on dual isotope approach in an agricultural watershed☆. Environmental Pollution **229**, 586, **2017**.
26. XIAO J., HAN X.X., SUN S.Q., WANG L.Q., RINKLEBE J. Heavy metals in different moss species in alpine ecosystems of Mountain Gongga, China: Geochemical characteristics and controlling factors☆. Environmental Pollution **272**, 115991, **2021**.
27. GIBBS R.J. Mechanisms controlling world water chemistry. Science **170**,870, **1970**.
28. WU C., WU X., QIAN C., ZHU G. Hydrogeochemistry and groundwater quality assessment of high fluoride levels in the Yanchi endorheic region, northwest China. Applied Geochem **98**, 404, **2018**.
29. GAILLARDET J., DUPRÉ B., LOUVAT P., ALLÈGRE C.J. Global silicate weathering and CO_2 consumption rates deduced from the chemistry of large rivers. Chemical Geology **159**, 3, **1999**.
30. XIAO J., JIN Z.D., WANG J. Assessment of the Hydrogeochemistry and Groundwater Quality of the Tarim River Basin in an Extreme Arid Region, NW China. Environmental Management **53** (1), 135, **2014**.
31. YANG Q.C., WANG L.C., MA H.Y., YU K., MARTÍN J.D. Hydrochemical characterization and pollution sources identification of groundwater in Salawusu aquifer system of Ordos Basin, China☆. Environmental Pollution **216**, 340-349, **2016**.
32. KAMMOUN S., TRABELSI R., RE V., ZOUARI K., HENCHIRI J. Groundwater quality assessment in semi-arid regions using integrated approaches: the case of Grombalia aquifer (NE Tunisia). Environ Monit Assess **190**, 87, **2018**.
33. LIN M.L., PENG W.H., GUI H.R. Hydrochemical characteristics and quality assessment of deep groundwater from the coal-bearing aquifer of the Linhuan coal-mining district, Northern Anhui Province, China. Environmental Monitoring and Assessment **188** (4), 1, **2016**.
34. DANIELE L., VALLEJOS Á., CORBELLA M., MOLINA L., PULIDO-BOSCH A. Hydrogeochemistry and geochemical simulations to assess water-rock interactions in complex carbonate aquifers: The case of Aguadulce (SE Spain). Applied Geochemistry **29**, 43, **2013**.
35. GUO Y., GUI H.R., WEI J.C., ZHANG Z., HU M.C., FANG P., LI G.P., GAO C., WANG X. Hydrogeochemistry of water in coal measures during grouting treatment of taoyuan mine, China. Groundwater **2020**.
36. QIU H.L., GUI H.R., SONG Q.X., YU J.W., ZHANG J.H. Hydrogeochemical characteristics of shallow groundwater in the Sunan coal-mining district, Northern Anhui province, China and its significance. Fresenius Environmental Bulleti **27** (11), 7853, **2018**.
37. GUI H.R., CHEN S. Isotopic geochemical characteristics of groundwater and its geological significance in Sunan mining area. Earth Science Frontiers **23** (3), 133, **2016**.
38. LIU S., TANG Z.H., GAO M.S., HOU G.H. Evolutionary process of saline-water intrusion in Holocene and Late Pleistocene groundwater in southern Laizhou Bay. Science of the Total Environment **607-608**, 586, **2017**.
39. BATSAIKHAN B., YUN S.T., KIM K.H., YU S., LEE K.J., LEE Y.J., NAMJIL J. Groundwater contamination assessment in Ulaanbaatar City, Mongolia with combined use of hydrochemical, environmental isotopic, and statistical approaches. Science of the Total Environment **765**, 142790, **2021**.
40. CHAO Y., YANG H.Q., WANG J.F., GUO J.Y., TANG X.Y., CHEN J.A. Combined use of stable nitrogen and oxygen isotopes to constrain the nitrate sources in a karst lake. Agriculture, Ecosystems & Environment **303**, 107089, **2020**.
41. Bureau of Quality and Technical Supervision of China (BQTS). National standard of the people's republic of China: quality standard for groundwater (GB/T 14848-2017). Beijing: Standards Press of China, **2017**.
42. RICHARDS L.A. Diagnosis improvement saline alkali soils. US Department of Agriculture Handbook. No. **60**, **1954**.
43. WILCOX L.V. Classification and use of irrigation waters. USDA. Circ 969, Washington, DC **1955**.
44. ERNESTO P.Z., ROGELIO L.R., THOMAS H., ALDO I.R., JÜRGEN M. Assessment of sources and fate of nitrate in shallow groundwater of an agricultural area by using a multi-tracer approach☆. Science of the Total Environment **470-471**, 855, **2014**.